Big Sky Carbon Sequestration Partnership – Phase II

TOPICAL REPORT

Enhanced Coal Bed Methane Recovery and CO$_2$ Sequestration in the Powder River Basin – Deliverable Gd10

Principal Author - Eric P. Robertson, Idaho National Laboratory

Performance Period – 10/1/2005 Through 12/31/10

Submitted by: Dr. Lee Spangler
BSCSP Principal Investigator and Director
Montana State University
P.O. Box 173905
Bozeman, MT 59717
spangler@montana.edu
http://www.bigskyco2.org
Phone: (406) 994-1658
Fax: (406) 994-3745

Big Sky Carbon Sequestration Partnership – Phase II

Enhanced Coal Bed Methane Recovery and CO₂ Sequestration in the Powder River Basin

Eric P. Robertson
Idaho National Laboratory

Abstract

Unminable coal beds are potentially large storage reservoirs for the sequestration of anthropogenic CO_2 and offer the benefit of enhanced methane production, which can offset some of the costs associated with CO_2 sequestration. The objective of this report is to provide a final topical report on enhanced coal bed methane recovery and CO_2 sequestration to the U.S. Department of Energy in fulfillment of a Big Sky Carbon Sequestration Partnership milestone.

This report summarizes work done at Idaho National Laboratory in support of Phase II of the Big Sky Carbon Sequestration Partnership. Research that elucidates the interaction of CO_2 and coal is discussed with work centering on the Powder River Basin of Wyoming and Montana. Sorption-induced strain, also commonly referred to as coal swelling/shrinkage, was investigated. A new method of obtaining sorption-induced strain was developed that greatly decreases the time necessary for data collection and increases the reliability of the strain data. As coal permeability is a strong function of sorption-induced strain, common permeability models were used to fit measured permeability data, but were found inadequate. A new permeability model was developed that can be directly applied to coal permeability data obtained under laboratory stress conditions, which are different than field stress conditions. The model can be used to obtain critical coal parameters that can be applied in field models.

An economic feasibility study of CO_2 sequestration in unminable coal seams in the Powder River Basin of Wyoming was done. Economic analyses of CO_2 injection options are compared. Results show that injecting flue gas to recover methane from CBM fields is marginally economical; however, this method will not significantly contribute to the need to sequester large quantities of CO_2. Separating CO_2 from flue gas and injecting it into the unminable coal zones of the Powder River Basin seam is currently uneconomical, but can effectively sequester over 86,000 tons (78,200 Mg) of CO_2 per acre while recovering methane to offset costs. The cost to separate CO_2 from flue gas was identified as the major cost driver associated with CO_2 sequestration in unminable coal seams. Improvements in separations technology alone are unlikely to drive costs low enough for CO_2 sequestration in unminable coal seams in the Powder River Basin to become economically viable. Breakthroughs in separations technology could aid the economics, but in the Powder River Basin, they cannot achieve the necessary cost reductions for breakeven economics without incentives.

Disclaimer

CONTENTS

FIGURES

TABLES

ACRONYMS

CBM	coal bed methane
CH_4	methane
CO_2	carbon dioxide
GHG	green house gas
PC	pulverized coal
N_2	nitrogen
ECBM	enhanced coal bed methane
PRB	Powder River Basin
RECOPOL	a CO_2 sequestration in coal project in Poland
INL	Idaho National Laboratory
O&M	operation and maintenance costs
NPV_{10}	net present value at a discount rate of 10%
ROI	return on investment
GOIP	gas originally in place
OIP	originally in place

Enhanced Coal Bed Methane Recovery and CO2 Sequestration in the Powder River Basin

1. Introduction

Sequestration of greenhouse gases (GHG) will likely be required in order to mitigate the climatological effects of rising GHG concentrations in the atmosphere. Carbon dioxide (CO_2) is a commonly emitted GHG resulting from the combustion of fuels such as coal, natural gas, oil, wood, and other similar fuels. Retrofitting stationary point sources such as pulverized coal (PC) power plants with technology to separate and capture CO_2 from flue gas emissions would allow the produced CO_2 to be collected and sequestered. In 2006, the U.S. generated 49% of its total electricity from coal-fired power plants (U.S. DOE, 2007a). These plants emitted roughly 1.91 Gt CO_2 in the same year (U.S. DOE, 2007b).

Coal seams have the capacity to adsorb large amounts of gases (especially carbon dioxide) because of their typically large internal surface area (30 to 300 m^2/g) (Berkowitz, 1985). Some gases, such as CO_2, have a higher affinity for the coal surfaces than others, such as nitrogen (N_2). Knowledge of how the adsorption or desorption of gases affects coal permeability is important, not only to operations involving the production of natural gas from coal beds but also to the design and operations of projects to sequester greenhouse gases in coal beds.

Injecting CO_2 into unminable coal seams has been proposed as a method to permanently sequester anthropogenic CO_2 emissions (Mathews et al., 2001; Steinberg, 2001; Schroeder et al., 2002; Zutshi and Harpalani, 2004; White et al., 2005). In addition to being potential sinks for CO_2 sequestration, many coal beds contain commercial quantities of adsorbed natural gas. Injecting CO_2 has been proposed as a method to enhance the production of methane from coalbed methane (CBM) operations in a process called CO_2-enhanced coal bed methane (CO_2-ECBM) (Puri and Yee, 1990; Pekot and Reeves, 2003; Busch et al., 2003; Prusty and Harpalani, 2004). The produced methane would create revenue that can offset the costs associated with the injection and sequestration of CO_2 in coal beds. In the CO_2-ECBM process, CO_2 is used to displace the adsorbed methane molecules and increase methane production without lowering reservoir pressure. As carbon dioxide is injected into a coal seam containing methane, the CO_2 molecules compete with the methane molecules for adsorption sites. Methane molecules detach from adsorption sites as CO_2 is injected into the coal due to a decrease in methane partial pressure in the free gas phase. The displaced methane ($CH_{4)}$ is then free to flow to a production well while the injected CO_2, which has a greater adsorption affinity than CH_4, is adsorbed onto the coal.

Fluid movement in coal is described by Darcy's Law as the gases flow through the natural fracture (cleat) system of the coal. Adsorption of gases by the internal surfaces of coal causes the coal matrix to swell and desorption of gases causes the coal matrix to shrink. The swelling or shrinkage of coal as gas is adsorbed or desorbed is referred to as sorption-induced strain. Sorption-induced strain causes the width of the coal cleats to change, thus changing the permeability of the coal. Modeling changes in coal permeability as a function of gas pressure has been the object of a number of papers (Gray, 1987; Sawyer et al. 1990; Seidle and Huitt 1995; Palmer and Mansoori 1998; Pekot and Reeves 2003; Shi and Durucan 2003), but modeling permeability changes in coal remains problematic (Robertson and Christiansen 2007).

Worldwide CO_2 storage capacity estimates in unminable coal seams range from 272 Gt CO_2 (Hendriks et al., 2004) to 350 Gt CO_2 (Stevens et al., 1998). Reeves (2003) estimated that the CO_2 storage capacity of unminable coal seams in the U.S. is 90 Gt CO_2 and he also estimated that unminable coal seams within the Powder River Basin of Wyoming and Montana are capable of storing 14 Gt CO2. According to these estimates of current output and storage capacity, the unminable coal seams within the

1

U.S. can provide 47 years of storage capacity for PC power plant CO_2 emissions, a significant potential storage medium for CO_2 emissions.

There have been a handful of field tests demonstrating the technical feasibility of using unminable coal beds to sequester CO_2 and stimulate the production of methane (White et al., 2005). These include the Tiffany unit in southern Colorado (Liang et al., 2003), the Allison unit in northern New Mexico (Reeves et al., 2003), the Medicine River coal seam in Alberta (Mavor et al., 2004), and the RECOPOL field project in Poland (van Bergen et al., 2003). These tests were not designed to evaluate the economic viability of sequestering CO_2 emitted from large anthropogenic point sources such a PC power plants. An economic analysis of CO_2 injection into unminable coal seams that accounts for the added benefit of increased methane production to help offset the cost of sequestering CO_2 emitted from PC power plants is needed.

2.   Study goals and objectives

The objective of this report is describe work at Idaho National Laboratory to study the interaction of CO_2 and coal and the applicability of using CO_2 to enhance study the economic feasibility of CO_2 sequestration in unminable coal seams in the regional setting of the Powder River Basin (PRB) of Wyoming and southern Montana (Figure 1). This specific setting was selected because of its large CO_2 sequestration potential, its national importance as the largest coal-producing basin in the United States, and its location within the Big Sky Regional Carbon Sequestration Partnership area.
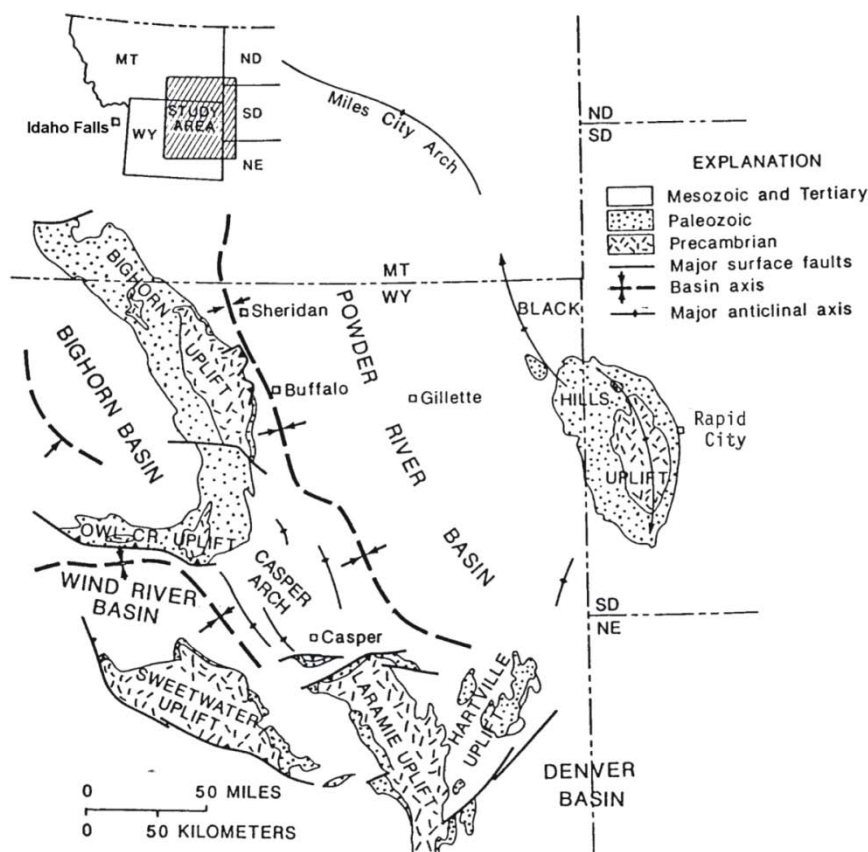
Figure 1. Map of Powder River Basin showing geographic location to INL in Idaho Falls and surrounding basin borders.

2

The Powder River Basin is located largely in northeastern Wyoming with a small portion extending into southeastern Montana (see Figure 1). The basin is a deep, northerly trending, asymmetric, mildly deformed trough, approximately 400 km long and 160 km wide. Its axis is close to its western margin, which is defined by the Bighorn Mountains uplift and the Casper arch. It is bordered on the south by the Laramie and Hartville uplifts and on the east by the Black Hills uplift. The northern margin is defined by the subtle northwest trending Miles City arch.

3.   Measurement of sorption-induced strain in coal

Sorption-induced strain can contribute up to 60% of the total change in coal permeability that occurs during the production of methane from coal beds (Robertson and Christiansen, 2008). Sorption of CO_2 can account for even more of the total permeability change during CO_2 sequestration or CO_2-ECBM operations. Published sorption-induced strain data is very sparse because the common method of collecting such data has been very cumbersome and time-consuming. INL pioneered the development of a new technique that is much quicker and reliable than the old method that obtained strain data by attaching strain gauges onto large blocks of coal.

A detailed methodology for taking the sorption-induced strain measurements is described in this section. The methodology is divided into 4 sections: 1) preparing coal samples and equipment, 2) use of equipment and the steps used to collect the appropriate data, 3) data reduction, and 4) plotting strain versus pressure curves.

3.1   Coal collection

A number of large coal blocks, roughly 1 ft^3 in size, were collected from coal mines in Utah and Wyoming. High-volatile bituminous coal from the Uinta-Peceance Basin was collected from the Gibson seam of the Book Cliffs coal field from an underground mine near Price, Utah. Subbituminous, low-contaminant coal from the Powder River basin was collected from the Anderson seam from an open-pit mine near Gillette, Wyoming. At the mine location, the Anderson seam was more than 100 feet thick. Proximate, ultimate, and heating-value analyses were subsequently performed on samples of the collected coal and are shown in Table 1.

Because most coals are sensitive to oxidation and because exposure of freshly mined coal to air at ambient temperatures for as little as a few days can adversely affect some properties such as heating value and tar yield (Berkowitz, 1994), care was exercised during the collection of the coal to limit exposure to air and to ensure that the samples remained as pristine as possible by following sampling procedures recommended by Gash (1991).

The Utah coal was taken from the conveyer belt carrying recently mined coal (less than one minute after contact by continuous miner machinery) as close to the active mine face as possible to limit oxygen exposure. Immediately after being taken from the conveyer, each sample was double wrapped in plastic bags and sealed by tape. Transporting the sample from the mine face to the surface via vehicle took from 5 to 20 minutes depending on the collection site. Upon reaching the surface, the samples were removed from the bags and placed under de-ionized water inside sealed containers for transport to INL facilities in Idaho Falls, Idaho. The Wyoming coal was collected from recently exposed walls (less than one day) from an open-pit mine where large boulders were broken open by hand to expose fresh coal. Smaller samples (roughly 1 ft^3 in size) of fresh coal were taken from these large boulders and immediately placed under water in sealed containers for transport to Idaho Falls, Idaho. Once at INL, the blocks were kept under water until needed.

3.2   Axial strain cell description

Previously used approaches for measuring coal strain are very time consuming and the resulting data can be difficult to interpret (Harpalani and Schraufnagel, 1990; Seidle and Huitt, 1995). Consequently, the data needed for understanding the change of coal permeability due to gas sorption are scarce. This

section details INL's development of an optical approach for measuring the strain of coal during gas sorption tests. With an optical approach, challenges of attaching strain gauges and passing electrical connections to a high-pressure chamber are entirely avoided. Furthermore, the size of the sample can be adjusted to minimize equilibration time, and multiple samples can be easily tested simultaneously. With this optical approach, we should be able to gather a suitable suite of strain data for testing permeability correlations.

Table 1. Properties of coal samples collected and used in this research as ascertained from various analyses on an "as received" basis.

	Anderson	Gilson
Location of seam	Wyoming	Utah
Coal rank	Subbituminous	High-volatile bituminous
Proximate Analysis wt%:		
Moisture	26.60	7.52
Ash	6.18	2.99
Volatile Matter	30.99	37.42
Fixed Carbon	36.23	52.07
Total	100.00	100.00
Ultimate Analysis wt%:		
Moisture	26.60	7.52
Hydrogen	2.08	3.86
Carbon	50.57	71.66
Nitrogen	0.43	1.36
Sulfur	0.27	0.49
Oxygen	13.87	12.12
Ash	6.18	2.99
Total	100.00	100.00
Heating Value, Btu/lb Measured	8,514	12,437
Vitrinite Reflectance, %	0.24	0.53

Figure 2 is a photograph of the axial strain vessel developed at INL (Robertson and Christiansen, 2007 (a) and (b)). Based upon the problems encountered using the proof-of-principle apparatus, a modified strain measurement apparatus was constructed. The main components of this refined system included a Jerguson cell, a removable multi-sample holder, and a digital filar microscope mounted directly to the pressure cell. The Jerguson cell was modified slightly by drilling-out the entrance and exit ports to allow for the passage of a ¼-inch rod. The multi-sample holder was fabricated out of a ¼-inch stainless steel rod and is easily removable from the pressure cell when samples need to be changed. A digital filar microscope manufactured by Gaertner Scientific, Inc. was mounted directly onto the pressure cell to more accurately measure changes in coal strain under different pressures and gas compositions. Mounting the microscope directly to the pressure cell eliminated the vibrational problems encountered with the proof-of-principle apparatus.
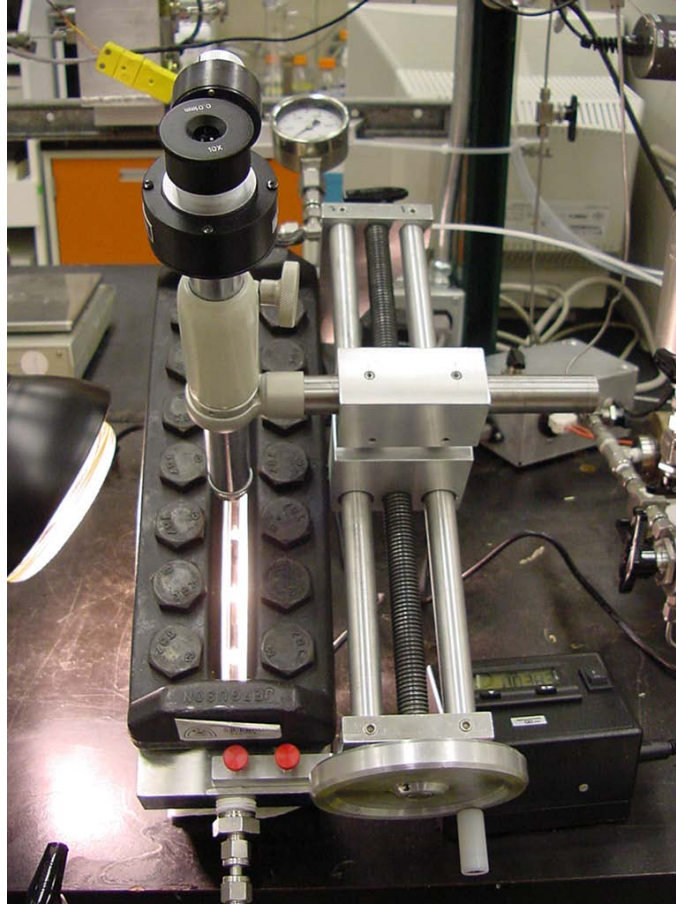
Figure 2. Photograph of the axial strain pressure cell without the temperature contol and accompanying insulation applied. The micrometer microscope is attached and a reflected light can be seen shining from behind through the sample beds cut into the 1/4-inch rod.

The rod holding the samples was centered in the pressure vessel by passing it through both the inlet and outlet ports of the pressure cell. The test gas could enter and exit the vessel through holes drilled through the center of the rod. A thermocouple was placed into the pressure vessel through the gas ports in the rod. Temperature in the vessel can be controlled with input from the thermocouple.

Six coal samples can be tested at the same time with this apparatus. The size of the samples is constrained by the dimensions of the sample "beds" machined into the rod. The maximum size is 1-inch in length by 5/32-inch in width by 1/8-inch in height. The sample beds have a solid bottom on which the coal samples rest except for the upper portion, which is machined completely through the rod to allow light to shine up from below and illuminate the coal sample.

A filar micrometer microscope with electronic readout was mounted directly to the Jerguson pressure cell to eliminate vibrations and to more accurately measure small movements. The microscope has a cross hair that moves across the field of view by means of a precision micrometer screw and reads to 0.0001mm with a 2.5mm range, which will accommodate up to a 10% elongation of the coal sample. For a sample of one inch in length, a 0.5% growth equates to an actual growth of 0.127mm, well within the specifications of the electronic readout.

A microscope holder was designed and fabricated that clamps directly to the pressure vessel. The microscope was mounted to the holding device; and by means of a hand-adjusted rotating screw, the microscope can be precisely moved along the entire length of the cell window. In this manner, multiple coal samples can be monitored during the same experiment. In Figure 2, one can see a number of the sample beds along with the microscope mounted onto the pressure cell.

3.3   Sample preparation for use in axial strain cell apparatus

The small samples used to measure strain were taken from these larger blocks using a rock saw cooled by deionized water. Coal pieces that fit in the machined beds must be cut and clipped from fresh coal chunks. This is done by first cutting thin rectangular strips of coal ¾ inches tall by ⅛ inches wide by however long they can be cut using a water cooled tile saw.

Once these strips are cut, smaller match-stick-size pieces are clipped so that they fit into the beds machined into a ¼-inch diameter solid stainless steel rod that is inserted into the axial strain vessel. The steel rod holding the coal samples can be seen inside the axial strain vessel in Figure 2. A pliers-like, hand-held tool is used for clipping these sample pieces. A control sample (cut from ⅛-inch stainless steel tubing makes an excellent control sample) usually occupies the lower-most sample bed and is used as a quality control sample. No measureable strain should be seen in the control.

Before the samples are inserted into the cell but after it is known that they are all the right size to fit into the small opening of the axial strain pressure vessel, the length of each sample is directly measured using a caliper and recorded in a laboratory notebook. Once the coal samples are loaded in the axial strain pressure vessel and before any other action (including temperature modification), measurements are collected on each of the samples to identify their initial end location with respect to a standard measuring mark.

A clear plastic strip with periodic marks about 1 mm apart is used as a standard against which sample strain are measured. The standard strip is laid on the outside of the pressure vessel directly above the coal samples on the sight glass and firmly secured to prevent subsequent movement. This strip is called the "measurement standard."

After the measurement standard is placed securely on the outside of the axial strain vessel and the samples (e.g. coal, stainless steel control, etc.) are placed within the vessel, the axial strain pressure vessel should be tilted to a fairly high angle – about 70 degrees from horizontal – to allow gravity to keep the lower end seated in the sample bed while keeping the upper end free to move when conditions are induced to cause strain.

3.4   Use of equipment and collection of appropriate data

A strain versus pressure curve is obtained by collecting sample length data at various gas pressures, converting the length data into strain, and then plotting strain versus gas pressure. Gases of interest include helium, nitrogen, methane, and carbon dioxide (others may be used also). Data points are collected at zero pressure (vacuum) and at a minimum of four other pressure values somewhat evenly spaced over the pressure range desired for the strain versus pressure curve.

3.4.1   Locating reference end points of samples

At this point, the location of each sample with respect to certain marks on the measurement standard is measured. This assumes that the filar microscope has already been mounted correctly to the pressure vessel. The microscope is focused on the free end of a sample, beginning with the lower-most sample. The crosshairs of the filar microscope are placed at the end of the sample by adjusting the horizontal adjuster (see Figure 3 for components of the filar microscope).

6
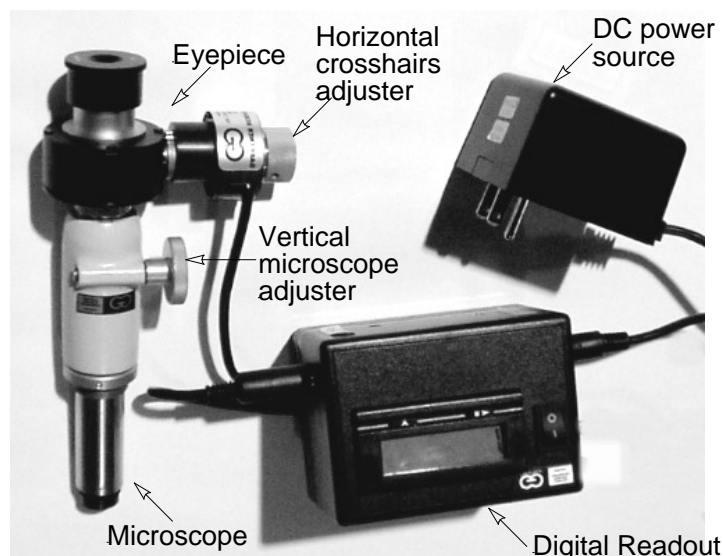
Figure 3. Components of the digital filar microscope used for measuring sorption-induced strain in coal.

The ends of the samples will not be smooth when seen through the microscope,; they will be irregular or jagged. Prominent points on each of the samples should be noted as reference end points. Drawing this reference end point for each sample in the laboratory notebook is a helpful way to remember it. The same reference point must be located and used repeatedly when measuring the strain throughout the strain experiments.

3.4.2   Measuring the distance between sample end and reference mark

The digital readout is zeroed when the crosshairs are on the reference end point of the sample. The microscope is then adjusted vertically (perpendicular to the plane of the direction of strain measurement) until it is refocused on the measurement standard on the outside of the pressure vessel.

The crosshairs are then adjusted until they are placed on the nearest mark of the measurement standard. This standard mark will be used for all subsequent measurements associated with this sample. The standard mark will be wavy, but a specific "wave" must be noted and used repeatedly for each sample. As with the sample reference end point, a drawing of the standard mark wave in the laboratory notebook is helpful in finding the point again.

The distance in millimeters between the end of the sample and the standard mark is read from the microscope's digital readout and recorded in laboratory notebook. This distance will be used to correlate subsequent changes in sample length to the original length measured by the calipers before the sample was put into the axial strain cell.

Once one of the sample measurements is taken, the entire microscope assembly is moved to the next sample by turning a threaded rod until the sample end comes into view through the microscope.

3.4.3   Temperature control

Strain measurements must be done at a constant temperature. Normal fluctuations in room temperature can cause significant errors in the collected data if temperature is not controlled. To control the temperature within the axial strain pressure cell, the cell is wrapped with an electrical heating strip and then with insulation. A thermocouple inserted into the axial strain pressure cell is used to record and

control the current *in situ* temperature. A temperature setting of 80 °F has been found to be high enough over room temperature of around 70 °F to overcome the effects of room temperature fluctuations. About 6 hours are required to stabilize the temperature inside the axial strain pressure cell from room temperature up to 80.0 °F.

3.4.4 Initialization pressure cycles

After the temperature has stabilized, the end location of each sample is read and recorded. Following this data reading, a hard vacuum is applied to the pressure chamber for 24 hours followed by pressurizing the chamber with helium. Strain measurements should be taken during these pressure cycles, which are repeated until constant strain values are obtained for each pressure state. When beginning a test with a different gas, a hard vacuum is applied to the samples for 24 hours and then pressurized with helium as a precautionary purge for 24 hours followed by another 24-hour vacuum period.

3.5 Data reduction: working with strain versus time data

After the strain data has been collected for each of the samples for a given gas, the strain versus pressure curve can be constructed. When the data are inputted into specially designed Excel™ spreadsheets, two plots are created: one plots the strain equilibration for each sample and the other plots the average strain versus time for all the samples. Figure 4 shows data for the average strain versus time for different adsorption pressures for methane and coal from the Trapper mine.
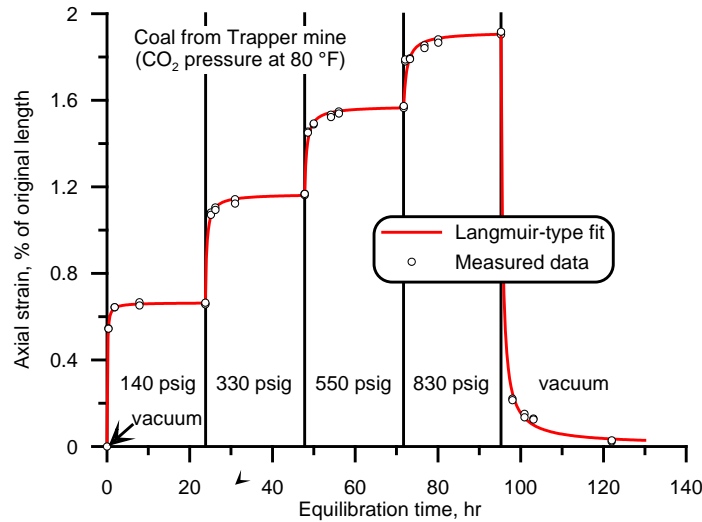
Figure 4. Average axial strain changes with respect to time for five coal samples from the Trapper mine in Colorado under various CO_2 gas pressures at 80 °F.

The measured data shown in this figure are shown as open circles, while the solid lines are "best fits" of the data, fit separately for each pressure regime. The best fit lines were obtained using a least squares subroutine for a modified form of the Langmuir equation that accounts for non-zero starting points:

$$S = S_1 + \frac{S_L(t - t_1)}{t_L + (t - t_1)},$$

where S is the calculated strain, S_1 is the initial strain at the beginning of the pressure regime, S_L is the Langmuir strain, t is the time in hours, t_1 is the time in hours at the beginning of the pressure regime, and

t_L is the Langmuir time. Both S_L and t_L were obtained by fitting the data using least-squares analysis with a Langmuir curve when both S_1 and t_1 are zero.

3.6   Plotting strain versus pressure curves

Langmuir parameters for the strain versus pressure curve are obtained by fitting the end point values of the data in Figure 4 for each pressure regime using the following Langmuir-type equation.

$$S = S_L \frac{p}{p + p_{S_L}},$$

where S is the freestanding axial strain, S_L is the Langmuir strain, p is the gas pressure, and p_{SL} is the Langmuir strain pressure.

Figure 5 shows an example of the axial strain for coal from the Trapper mine in Colorado for various gases as a function of pressure at a constant temperature of 80 °F. The calculated data shown in this figure are shown as open circles, while the solid lines are "best fits" of the data obtained using a least-squares approach with the above Langmuir-type equation.
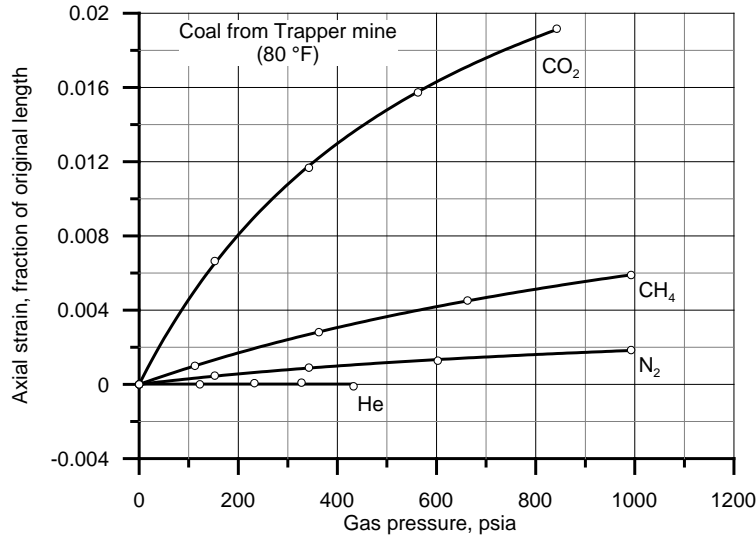
Figure 5. Axial strain for coal from the Trapper mine in Colorado for various gases as a function of pressure at a constant temperature of 80 °F. For each of the gas datasets, the data are fitted with the Langmuir equation.

Description of the procedures and equipment used to obtain free standing, axial strain, sorption-induced strain was included in this report in order to show the rigor used during data acquisition. Obtaining the raw data necessary to construct the relationships shown in Figure 5 requires about five weeks. Constructing this same plot from data obtained using traditional strain gauges would require about one year due to the long stabilization times associated with the required larger samples. These data are necessary to accurately model permeability changes in coal due to sorption (desorption and/or adsorption) of gases that occurs during geologic CO_2 sequestration activities.

4. Modeling sorption-induced coal permeability changes

All permeability measurements were made in INL laboratories at 80°F with gas as the flowing fluid using 2-in. diameter cores cut parallel to the bedding planes. The cores were cut from the larger blocks of coal using deionized water as the cooling/lubricating fluid. Some of the cores "fell apart," either while cutting the cores or while attempting to remove them from the core bit, but persistence and care while drilling resulted in many good cores to use for the flow tests. The cores were stored in small, sealed containers under deionized water until used in the experiments. Figure 6 is a photograph of the trimmed ends of some of the Gilson-seam cores and is shown to give the reader an idea of a typical cleat system associated with these cores.

Figure 6. Photograph of trimmed ends from Gilson-seam coal cores 2 in. in diameter. Note the irregular cleat system associated with this coal.

A hydrostatic-type core holder was used for the permeability experiments. The flowing gas was supplied by pressurized gas cylinders, and the flow rate was controlled by adjusting both the cylinder regulator and a metering valve upstream of the core holder. A backpressure regulator was used to apply a minimum of 100 psia of pore pressure to minimize the Klinkenberg effect of gas-permeability measurements. Upstream and differential pressures were made using pressure transducers. A flow meter was placed directly downstream of the backpressure regulator.

4.1 Measurement of permeability data

A description of the experimental procedure used to collect permeability data is discussed by Robertson and Christiansen (2007). Using the permeability apparatus, permeability was measured using nitrogen, methane, and carbon dioxide as the flowing fluids for two coals described in Table 1. The results of these permeability tests are shown in Figure 7 (a) and (b).

4.2 Comparison of permeability data to common models

Being able to model and accurately predict permeability changes is an important and vital capability that is necessary to the proper design of CO_2-ECBM and for CO_2 sequestration in unmineable coal seams. Three well-known permeability models were selected from the literature to model the laboratory permeability data (see Figure 7): Seidle and Huitt (1995), Palmer and Mansoori (1998), and Shi and Durucan (2003).
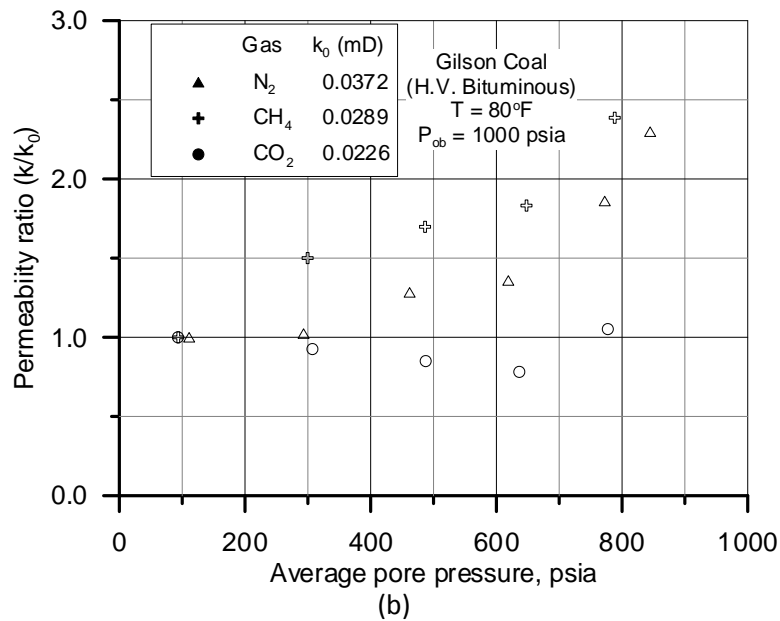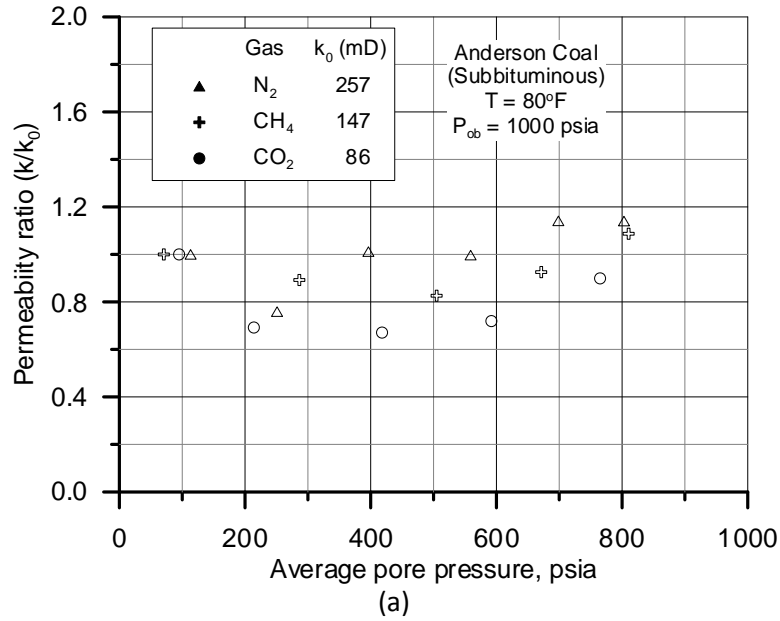
Figure 7. Permeability as a function of pore pressure for three different pure gases for (a) Anderson coal and (b) Gilson coal.

Figure 8 shows the three models applied to the measured permeability data. None of the three coal permeability models did a very good job matching actual permeability data for all six cases. However, two of the models (Shi-Durucan and Palmer-Mansoori) did relatively well matching the nitrogen permeability data.

It should be noted that the laboratory permeability measurements were made under hydrostatic conditions where the confining pressure was equal in all directions, whereas the models selected to match that data were derived for matchstick-type fractured geometry under uniaxial strain conditions, thought to

more closely describe field conditions. Even though the models might not be totally applicable to laboratory permeability measurements, they are applied in this work to define a starting point for potential modifications or improvements. If one could develop a model to accurately predict laboratory permeability changes in sorptive-elastic material, such as coal, the model could be used as a tool to determine coal properties of use in field simulations.
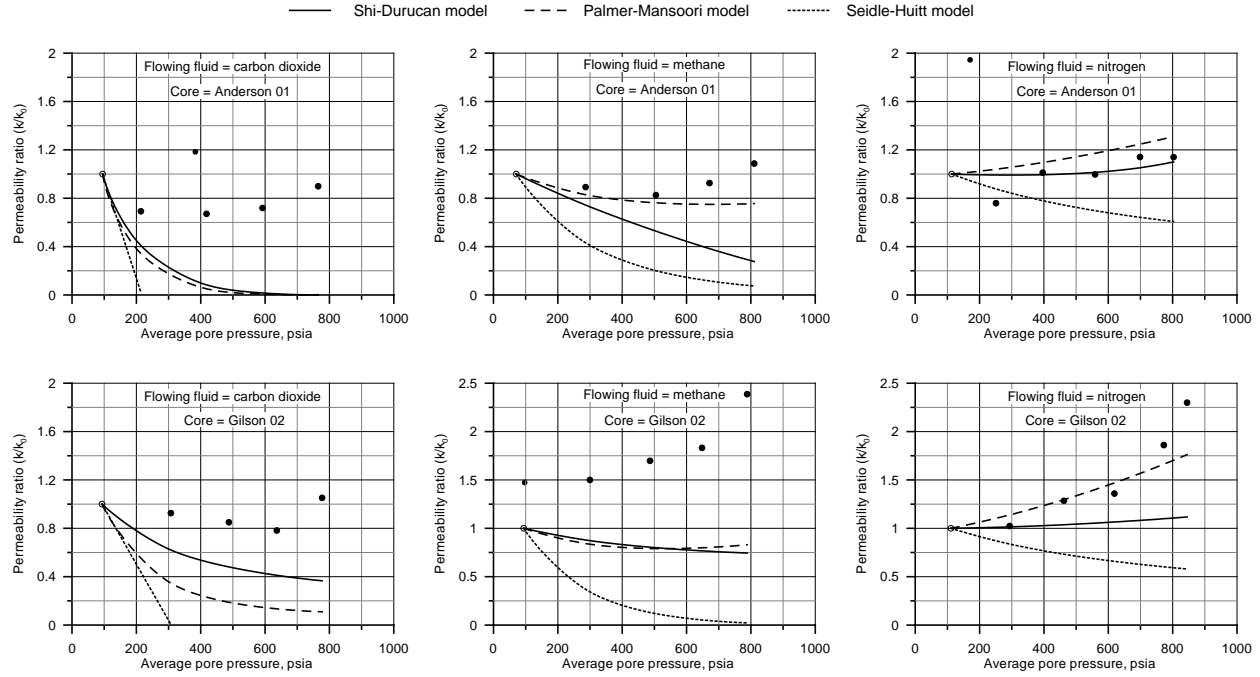
Figure 8. Model comparisons for two coal cores and three flowing gases. For all experiments, confining pressure was 1000 psia and temperature was 80°F.

4.3   Development of new permeability model for laboratory conditions

A new model was derived (Robertson and Christiansen, 2008) that describes the permeability behavior of a fractured, sorptive-elastic media, such as coal, under typical laboratory conditions where common radial and axial pressures are applied to a core sample during permeability measurements. The new model can be applied to fractured rock formations where the matrix blocks do not contribute to the porosity nor to the permeability of the overall system, but where adsorption and desorption of gases by the matrix blocks cause measurable swelling and shrinkage and thus affect permeability. The derived model is represented by the following equation:

$$\frac{k}{k_0} = e^{3\left\{c_0\frac{1-e^{\alpha(p_p-p_{p0})}}{-\alpha}+\frac{3}{\phi_0}\left[\frac{1-2\nu}{E}(p_p-p_{p0})-\frac{S_{max}p_L}{(p_L+p_{p0})}\ln\left(\frac{p_L+p_p}{p_L+p_{p0}}\right)\right]\right\}},$$

where k is measured permeability, k_o is the initial permeability of the coal core, c_0 is the initial fracture compressibility, α is the fracture compressibility change rate, p_p is the pore pressure, p_{p0} is the initial pore pressure, ϕ_0 is the initial porosity, ν is Poisson's ratio, E is Young's modulus, S_L is the Langmuir strain, and p_L is the Langmuir pressure.

12

4.3.1 Discussion of new model

Understanding the dynamics of the physics involved with changes in permeability in sorptive-elastic media, such as coal, is of vital interest to those involved with optimizing production from coal bed natural gas fields, sequestering carbon dioxide in coal beds, or producing natural gas from some shale formations. Laboratory experiments can be designed to enlighten the engineer as to what processes contribute to project success and how they can best be manipulated to increase recovery or economic viability. The equations derived above are based on the conditions encountered in laboratory experiments designed to calculate permeability. An accurate understanding of how permeability can change during production and injection operations is very important. This present model should help researchers to better understand the processes that influence permeability and to derive realistic values of important parameters, such as fracture compressibility, initial porosity, and elastic mechanical moduli, that need to be included in field-wide reservoir simulations.

4.3.2 Use of model as tool to predict key coal properties

This model has been appropriately derived for conditions frequently used in laboratory-measured permeability test on coal samples. Key, hard-to-measure coal properties can be determined by fitting laboratory-measured permeability data with this model. For example, Young's modulus and Poisson's ratio are important parameters needed to accurately forecast permeability behavior during coalbed methane operations; yet, these values are difficult to measure and general values are typically used. If initial porosity, fracture compressibility, and sorption-induced strain were all fairly well known, the elastic moduli (Young's modulus and Poisson's ratio) could be determined by varying their values until the model reached a reasonable fit of the permeability data. These model-determined values could then be used in field-scale models to improve permeability forecasts.

4.3.3 Relative contribution of terms in permeability model

The permeability model given above contains three terms representing the contribution of fracture compressibility, mechanical elastic matrix strain, and sorption-induced matrix strain to fracture width and permeability change. One might suspect that one factor could be more important to permeability change than the others or that one of the three could be a relatively small contributor to permeability change. Figure 9 (a) shows the change in permeability ratio caused by contribution of the three components of the permeability model and Figure 9 (b) shows the relative contribution of each of the terms to the total permeability ratio calculated by the model.
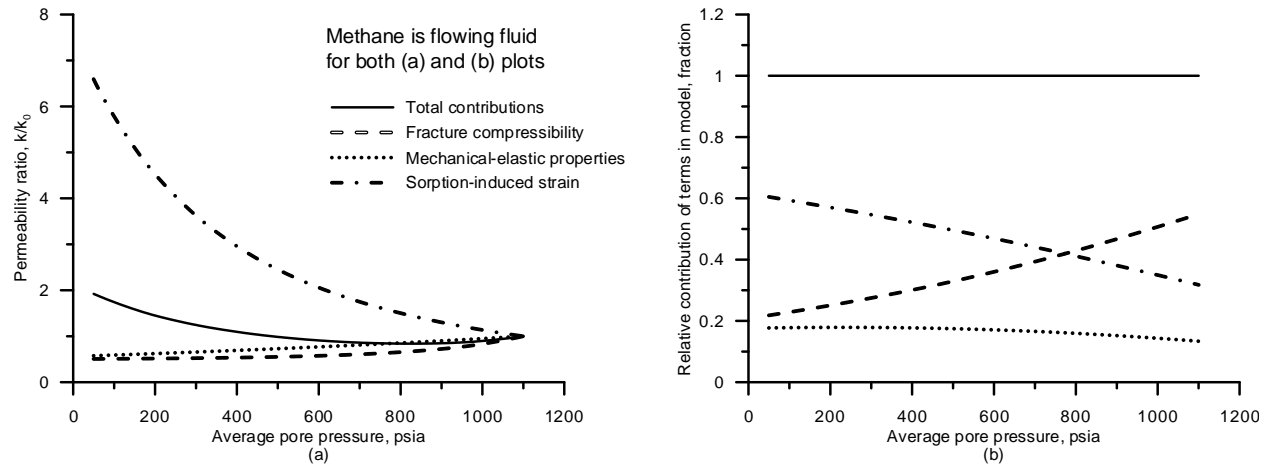

Figure 9. Plots showing the relative contributions of model terms to model output.

13

4.3.4 Discussion of new model

The new permeability model can be used to model permeability changes in coal (and other substrates, such as sorptive shale) as stresses change. In addition, the model can be used to model permeability changes caused by the injection of other gases, such as carbon dioxide for sequestration in coal.

Sensitivity analysis of the model found that each of the input variables can have a significant impact on the outcome of the permeability forecast as a function of changing pore pressure (Robertson and Christiansen, 2008). However, the permeability model can be used as a tool to determine some of the parameters by curve-fitting laboratory-generated permeability data. These model-determined values could then be used for field simulations with a greater degree of confidence.

The new model reduces the effect of sorption-induced strain on permeability compared to two "field" permeability models.

5. Economic evaluation

The methodology for performing an economic evaluation of CO_2 sequestration/CO_2-ECBM outlined in this section of the report could be applied to other basins around the world using costs and coal characteristics specific to the basin of interest. The Wyodak PC power plant located near Gillette, Wyoming, in the PRB was utilized as the CO_2 point source and the deep, unminable Wyodak-Anderson coal zone some 80.5 km from the power plant was chosen as the hypothetical injection site. Unminable coal was defined as coal below a depth of 304.8 m (Nelson et al., 2005).

Wyoming has several large point source carbon dioxide emitters with total emissions of about 57 Mt CO_2 per year (Robertson, 2007). Table 2 lists the coal-fired power plants in the state, which account for over 80% of Wyoming's total point source emissions with the balance coming from trona processing, petroleum refining, and cement manufacture.

Table 2. Wyoming coal-fired power plants.

Plant	County	Capacity (MW)	CO₂ Emissions (Tons/yr)
Jim Bridger	Sweetwater	2,120	18,576,558
Laramie River Station	Platte	1,650	14,442,863
Dave Johnston	Converse	762	7,362,207
Naughton	Lincoln	700	6,012,586
Wyodak	Campbell	335	3,762,075
Neil Simpson II	Campbell	114	1,264,726
Wygen1	Campbell	90	900,000

The Wyodak facility was selected as the specific CO_2 point source for this analysis because of its location in the Powder River Basin, its proximity to potential geologic sequestration sites, and its relatively average size compared to other power-generation facilities within the state. The Wyodak PC power plant generates 335 MW of net power and consumes approximately 5500 Mg/D of Powder River Basin coal. The plant was built in 1978, with an expected life of 45 years and a thermal efficiency of 29.3%. The coal used in the plant has an average heating value of 7727 Btu/lb (17.934 kJ/g) and an average carbon content of 46.2 wt.% (Robertson, 2005).

About 613.6 m³/s of flue gas at atmospheric pressure and 85 °C flows through the emissions stack. Nitrogen and carbon dioxide respectively account for 67.0 mol% and 11.8 mol% of the flue gas discharged from the Wyodak PC power plant (Table 3). On average, 9344 Mg CO_2 are emitted each day from the Wyodak facility (Robertson, 2007).

Table 3. Flue gas composition of Wyodak PC power plant.

Flue gas component	Concentration
N_2	67.0%
CO2	11.8%
O_2	12.0%
H_2O	8.0%
CO	300 ppm
SO_2	180 ppm
NO_x	150 ppm

The Wyodak-Anderson subbituminous coal zone is the largest coal zone in the Powder River Basin. The approximate extent of the unminable portion of the Wyodak-Anderson coal zone in the PRB is the area encompassed by the white line drawn in Figure 10. The maximum depth of the Wyodak-Anderson coal zone is about 2500 ft (762 m) near the basin axis. Defining unminable coal as all coal below 1000 ft (305 m), the average depth of the unminable coal in the Wyodak- Anderson coal zone is 1500 ft (457 m).
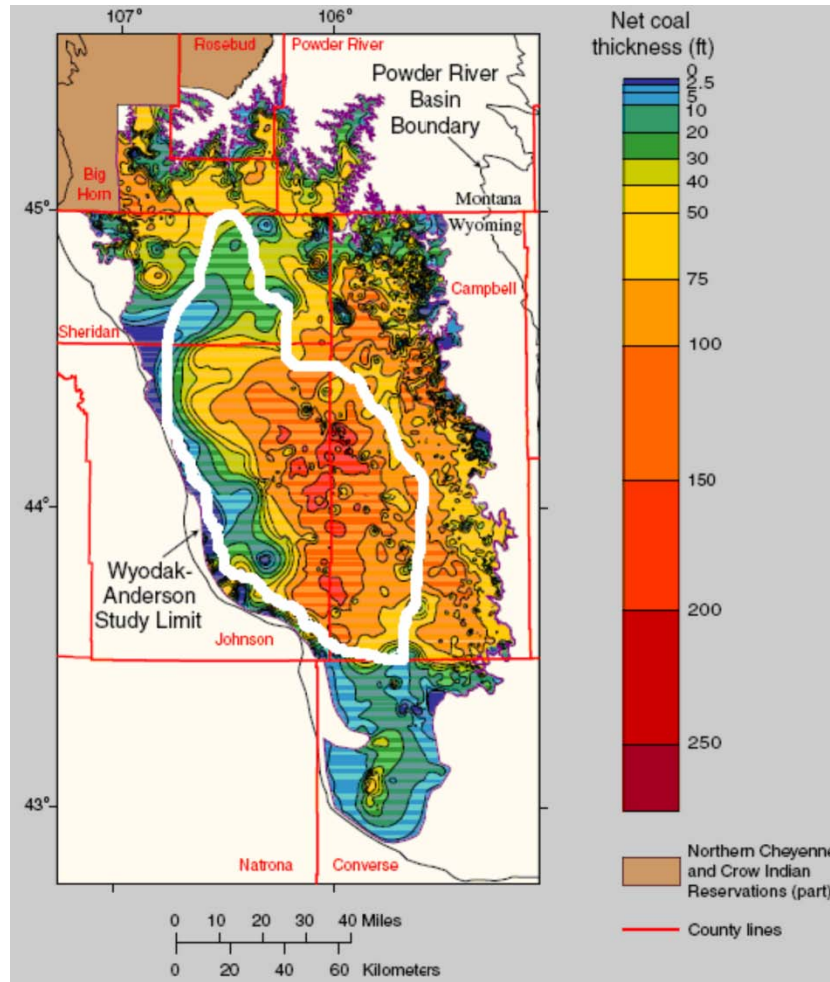
Figure 10. Wyodak-Anderson net coal isopach map. The area encompassed by the white line represents the approximate unminable coal area overlain by over 1000 ft (304.8 m) of overburden.

The thickness of the unminable coal is between 75 ft (23 m) and 200 ft (61 m) (Figure 10). A value of 100 ft (30 m) was used in the analysis as a representative thickness. Nelson et al. (2005) estimated the CO_2 storage capacity for the unminable coal in the Wyodak-Anderson coal zone of the PRB to be 101.2 trillion cubic feet (5.34 Gt CO_2). Based on this capacity, the unminable portion of the Wyodak coal zone would be capable of sequestering over 3000 years of CO_2 from the Wyodak power plant at current output levels.

5.1   Approach

The majority of coal bed reservoirs are initially saturated with water and whether the adsorbed methane is produced by pressure depletion or by the aid of gas injection (CO_2 sequestration), much of the water will be pumped from the coal before the majority of the adsorbed gas can be produced. As a base case, the economic feasibility of traditional methane production without any gas injection to enhance production was analyzed. Two gas injection scenarios were also analyzed. These are broadly described as (1) injecting a separated CO_2 stream from emissions from the Wyodak PC power plant into an unminable coal seam in the Powder River Basin; and (2) injecting unseparated flue gas (including the entrained CO_2).

Each scenario was analyzed assuming a 5-spot pattern on 320-ac (129.5-ha) well spacing. For the two injection scenarios, a 1:1 ratio of injection and production wells was employed as well as a 50-mile (80.5-km) pipeline to transport the injection gas from the Wyodak plant to the sequestration site. Additionally, each scenario required the drilling of shallower wells for the disposal of produced water.

Table 4. Base values of input parameters used to compare economics of carbon dioxide sequestration scenarios.

| Input Variable	Value Base	Minimum	Maximum	Units
Length of pipeline to transport gas to sequestration site	50	5	50	miles
Depth from surface to coal seam	1,500	1,000	2,000	ft
Capacity of nitrogen separation facility	300	270	330	Mcf/D
Capital costs				
Capex associated with water disposal	36,400	35,000	40,000	$/well
Capex for nitrogen separation facility	500	400	550	$/Mcf/D
Mineral rights and permitting	120,000	108,000	132,000	$/320 ac
Operating costs				
Injected gas transportation tariff	9.17E-3	8.25E-3	10.09E-3	$/Mcf/mile
carbon dioxide/flue gas separation	42.00	20.00	50.00	$/ton
Water disposal	0.10	0.09	0.11	$/bbl
O&M for nitrogen separation	0.40	0.35	0.50	$/Mcf
Miscellaneous items				
Natural gas price	8.00	6.00	12.00	$/Mcf
Price differential between national average and Powder River basin wellhead	-1.00	-1.50	-0.50	$/Mcf
Inflation rate	0.03	—	—	
Royalty rate	0.125	—	—	
Ad valorem & severance tax rate	0.12	—	—	
Federal income tax rate	0.35	—	—	
Discount rate	0.10	—	—	

5.2 Economic model description

The economics of each scenario were compared using probabilistic discounted cash flow, after-tax analysis for the life of the projects. A probabilistic approach was employed to evaluate critical and significant input variables. Input parameters were assigned triangular distributions by assigning minimum values, most likely values, and maximum values. Revenues for the scenarios were generated based on the sale of produced methane from the coal seams. Costs include well drilling costs, injection gas purchase cost, water disposal costs, taxes, etc. Table 4 is a summary of the input parameters used in the economic evaluations showing their base values as well as their minimum and maximum values used for the triangular distributions. These parameters are further discussed in the following section.

5.2.1 Forecast of fluid production rates

Commercial CBM reservoir simulation software was used to simulate the production response from an unminable coal seam in the Powder River Basin resulting from the injection of carbon dioxide and flue gas. Important reservoir parameters and their values used for the simulation are shown in Table 5. Isotherms for carbon dioxide, methane, and nitrogen (Figure 11) are used to calculate production and storage as a function of *in situ* pressure within a particular coal seam.

Table 5. Key parameters used for simulation of CO_2-sequestration in PRB unminable coal seams.

Reservoir parameter	Value	Units
Depth to top of coal seam	1500	ft
Coal thickness	100	ft
Well spacing	320	acre
Initial reservoir pressure	650	psia
Permeability	50	md
Porosity	0.02	fraction
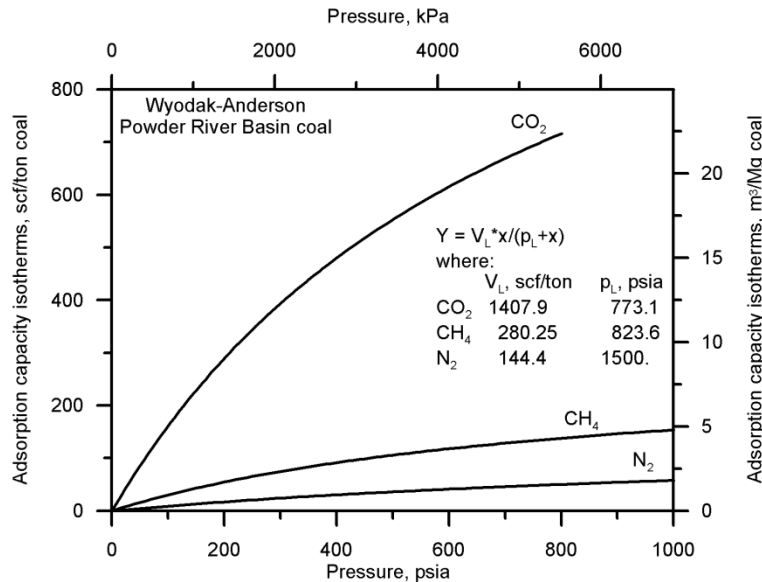
Figure 11. Gas capacity isotherms for carbon dioxide, methane, and nitrogen for the Wyodak-Anderson coal seam used in the reservoir simulation.

Simulated methane production curves for the three scenarios (Figure 12) show that production is retarded in the two ECBM scenarios. This retardation is primarily due to the large volume of water being driven from the injector towards the producing well. The water inhibits methane desorption from the coal matrix and also impedes the flow of gas through the cleat system.
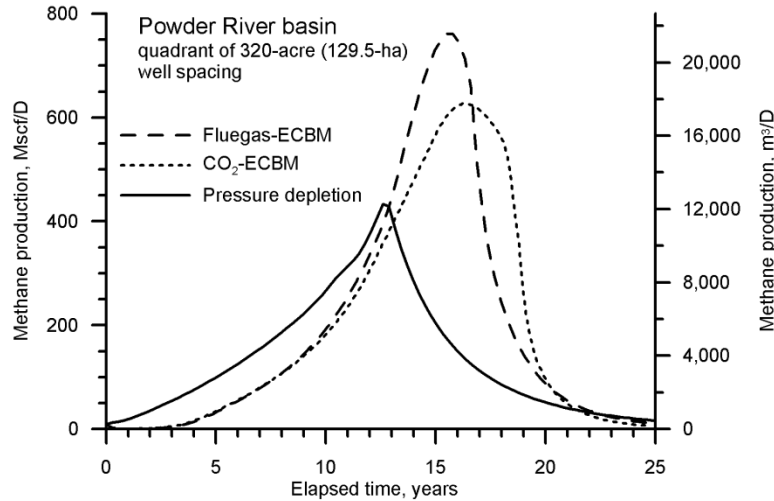
Figure 12. Methane production curves for the three scenarios analyzed.

5.2.2   Mineral rights

Mineral rights and permitting for the 320-acre (129.5-ha) spacing was estimated to be $120,000 following the example of Bank and Kuuskraa (2006).

5.2.3   Injection and production wells

The capital costs for these wells were calculated according to the methodology outlined by Bank and Kuuskraa (2006), for CBM wells in the Powder River Basin. For well depths (D_w) between 1000 ft (305 m) and 3000 ft (914 m), drilling cost (C_D) was calculated using:

$$C_D = 110D_W - 5500.$$

At a depth of 1500 ft (457 m) to the coal seam, the cost of the wells were estimated to be $159,500 per well.

5.2.4   Produced water disposal costs

Options for produced water disposal include surface discharge, infiltration impoundment, shallow underground injection, and deep underground injection. Treatment options that would allow surface discharge of the produced water include technologies such as reverse osmosis and ion exchange. A shallow underground injection scheme was chosen as a suitable option for the disposal of produced water for the three scenarios considered in this paper. Capital costs for this water disposal option were estimated to be $36,400 and operating and maintenance (O&M) costs were estimated to be $0.10/bbl ($0.63/m^3) of produced water (Bank and Kuuskraa, 2006).

5.2.5 Transportation costs for injection-gas

The transportation cost for the injection gas was incorporated into a pipeline tariff and includes the gas compression cost. The pipeline tariff was calculated Thomas et al. (1996):

$$T = \frac{3.35 C_p}{V},$$

where T is the pipeline tariff in $/m^3/km, C_p is the capital cost of the pipeline construction in $/km, and V, in m^3, is the total volume of fluid transported through the pipeline over a 10-year period. The tariff calculation applies to both injection scenarios. Robertson (2007) reported that a CO_2 pipeline transporting gas separated from the Wyodak power plant would cost about $522,000/km with a throughput of 2,383,000 m^3/D. Using these costs, the tariff for the CO_2 injection scenario was calculated to be $0.000201/m^3/km.

5.2.6 CO_2 separation costs

To obtain a CO_2 stream for the CO_2 injection scenario, a CO_2 separations unit was placed at the Wyodak plant. Three CO_2 separation technologies were analyzed for the treatment of the Wyodak flue gas stream, which were chemical absorption technology, separation by adsorption, and membrane separation. The analysis concluded that chemical absorption technology was the most economic separation technology for the specific requirements and captured roughly 50% of the CO_2 emitted (Robertson, 2007). The breakeven sale price of the CO_2 separated from the plant was determined to be $42/ton ($46.3/Mg).

5.2.7 Costs to separate nitrogen from produced gas

Under the flue gas injection scenario, both nitrogen and carbon dioxide were injected into the coal seam. The nitrogen has a lesser affinity for adsorption onto the coal surfaces than either methane or carbon dioxide. As a result, the nitrogen component in the flue gas travels through the coal seam and reaches the producing well sooner than the carbon dioxide necessitating the installation of a nitrogen separations unit at the production well to remove the nitrogen from the produced gas to improve the product to pipeline quality. Bomberger et al. (1999) discussed various technologies for nitrogen removal from natural gas and reported that capital costs for nitrogen removal from natural gas streams were about $17.66/m^3/D with operating costs of about $0.0141/m^3. These values were used in the economic evaluation of the flue gas injection scenario.

5.2.8 Other input variables

The natural gas price forecast according to the Energy Information Administration (EIA, 2007) is projected to be fairly flat. The analysis assumes a flat natural gas price of $8.00/Mscf ($0.2825/m^3) in the U.S., with a $1.00/Mscf ($0.0353/m^3) discount that accounts for the price differential between wellhead gas in the Powder River Basin and the national average.

The total income tax rate for the analyses was estimated to be 35%, the royalty rate was estimated to be 12.5%, and the combined state severance and ad valorem tax rate was estimated to be 12%. Inflation was estimated to be 3% and a discount rate of 10% was used for the discounted cash flow analysis.

5.3 Results and discussion

Economics of the three production scenarios (no gas injection, flue gas injection, and CO_2 injection) were compared using deterministic discounted cash flow analysis. Further analysis of the CO_2 injection/ sequestration scenario was done using probabilistic or Monte Carlo techniques.

5.4   Deterministic comparisons

Two economic parameters were used to compare the scenarios: net present value at a discount rate of 10% (NPV_{10}) and rate of return on investment (ROI). Economic analyses using the most likely values show large disparities between the results of the three evaluated production scenarios (Table 6). The NPV_{10} of the no-gas-injection scenario was $1.55 million, the NPV_{10} of the flue-gas-injection scenario was −$0.81 million, and the NPV_{10} of the CO_2-injection scenario was −$36.2 million. The most economically advantageous avenue would be to produce the methane from the coal bed without any additional "enhancement" by the injection of either flue gas or carbon dioxide. At current natural gas prices and costs to capture CO_2 from anthropogenic sources, CO_2-ECBM is not expected to be profitable for scenarios similar to those analyzed in this paper.

Table 6. Deterministic economic results using most likely values for input parameters for three scenarios analyzed.

Scenario	Length of project, yr	NPV_{10}, $(millions)	ROI, %	Methane recovered, % GOIP	CO_2 sequestered, tons
No gas injection (pressure depletion)	26	1.55	24.3	71.7	0
Flue gas injection (flue gas-ECBM)	17	-0.81	5.4	70.2	147,000
CO_2 injection (CO_2-ECBM)	19	-36.2	0	88.2	6,860,000

The projected termination date of the no-gas-injection scenario is 26 years after project initiation with recovery of 72% of the methane originally in place (OIP) and no carbon dioxide sequestered. Because of large amounts of nitrogen in the produced gas, the flue-gas-injection scenario is terminated after 17 years during which 70% of the methane OIP were recovered and 147,000 tons (133,600 Mg) of CO_2 were sequestered. The CO_2-injection scenario was terminated after 19 years due to CO_2 breakthrough at the production well with recovery of 88% of the methane OIP and 6,857,000 tons (6,233,600 Mg) of CO_2 sequestered.

Although the economic results suggest that the flue gas-ECBM scenario is close to being profitable, the amount of CO_2 sequestered is small and does not significantly contribute to the need to sequester CO_2 in large quantities. Therefore, flue gas injection scenarios should be viewed as an enhanced CBM method and not as a realistic option for CO_2 sequestration. Out of the two injection scenarios analyzed, only the scenario injecting pure CO_2 into the coal seam is a true CO_2 sequestration option. This option, although uneconomic without forced or voluntary subsidies, effectively recovers methane and also sequesters 6.9 million short tons (6.2 Mt) of CO_2 per quadrant of a 320-ac (129.5-ha) well-spacing pattern.

5.5   Monte Carlo analysis of CO_2 injection scenario

Monte Carlo analysis was used to determine the distribution of net present value for the CO_2 injection scenario by employing the triangular distribution assigned to each input variable. The resulting distribution of NPV_{10} for the CO_2 injection scenario is shown in Figure 13, which ranges from -$43 million to -$6 million and has a mean value of -$29.3 million.
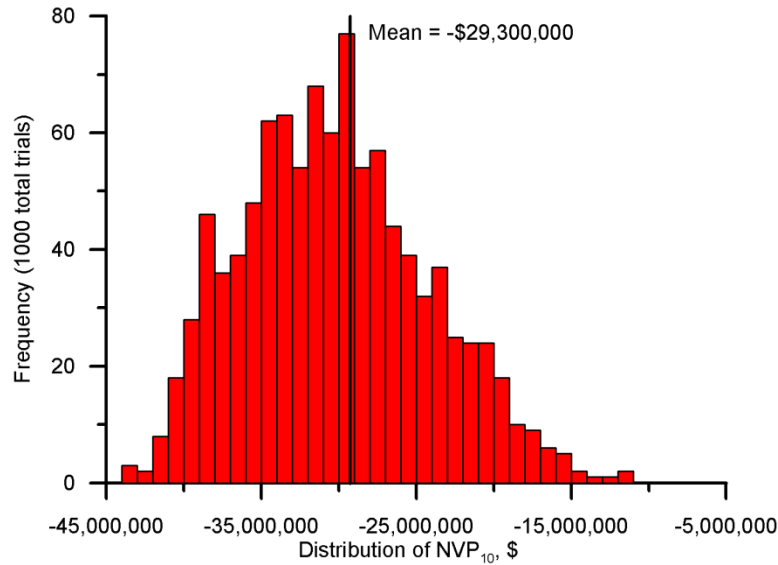
Figure 13. Probabilistic net present value (NPV$_{10}$) of the CO$_2$ injection scenario.

5.5.1 Sensitivity analysis

A sensitivity analysis was performed on the CO$_2$ injection scenario to determine the input parameters causing the most variability in the net present value. Correlation coefficients, which represent the degree to which an input variable and net present value change together, were calculated for each variable and normalized with respect to 100%. A negative correlation coefficient means that as the input variable increases, the resulting net present value tends to decrease; while a positive coefficient signifies an increase in NPV with an increase in the input variable. The correlation coefficients of the five input variables with the most impact on the net present value are plotted in Figure 14. The input parameter with the greatest effect on economic viability is the cost to separate CO$_2$ from flue gas.

5.5.2 Total CO$_2$ cost to sequestration projects

The total cost of the CO$_2$ to the sequestration project is the combination of costs to separate it from flue gas and costs to transport it to the sequestration site (including compression costs). Data shown in Figure 14 identify the cost to separate and capture CO$_2$ from the flue gas stream of the Wyodak PC power plant as the most critical input variable for the economic evaluation of the CO$_2$ injection project in the Powder River Basin because it has the greatest impact on the net present value of the scenario.

CO$_2$ separation and capture has the greatest impact on net present value not only because of its large cost, but also because of its large uncertainty range. The most likely value of \$42/ton (\$46.2/Mg) for this cost was based on a site-specific estimate of retrofitting currently commercial CO$_2$ separation technology. The minimum value for this cost of \$20/ton (\$22/Mg) was based on future improvements to CO$_2$ capture and separation technology that would dramatically reduce this cost to about one-half of its current value; while the maximum value of \$50/ton (\$55/Mg) was selected assuming no future technological improvements.

Assuming that the CO$_2$ separation cost is \$42/ton (\$46.2/Mg) and also including the transportation cost of \$0.46/Mscf (\$0.0162/m^3) for a 50-mile (80.5-km) pipeline, the total cost of the CO$_2$ is \$3.03/Mscf (\$0.107/m^3). If the separation cost were reduced to \$20/ton (\$22/Mg) of CO2, the total cost of the CO$_2$ would be \$1.68/Mscf (\$0.0593/m^3).

21
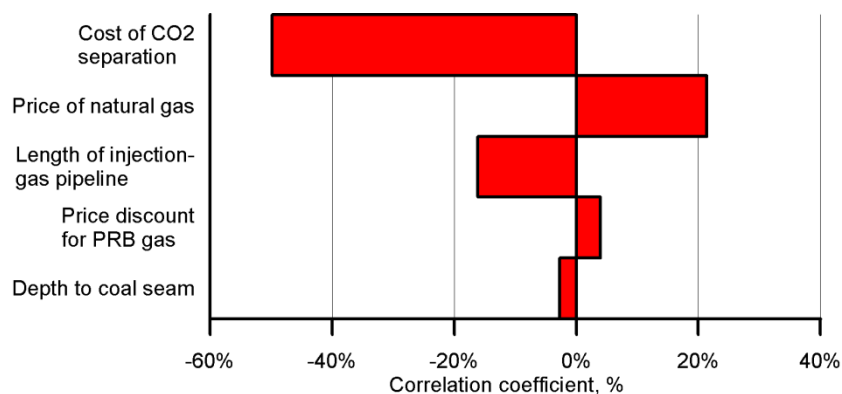
Figure 14. Correlation coefficients for the five input variables with the most impact on the net present value of the CO_2 injection scenario.

The economic model was evaluated to determine the effect of reducing the CO_2 separation cost to $20/ton ($0.706/Mg) through technological innovation. The resulting NPV_{10} distribution of the scenario was still negative for all cases. This information indicates that, at least for this specific location, injecting CO_2 into an unminable coal seam would most likely never be profitable without some additional economic driver being present. Powder River Basin coal has low methane content – typically around 30 scf/ton (0.9365 m^3/Mg) of coal (ALL, 2004) – compared to other basins containing higher rank coal such as the San Juan Basin with methane content of around 400 scf/ton (12.48 m^3/Mg) of coal (ALL, 2004). The low volumetric recoveries for the Powder River Basin are not sufficient to offset the costs of CO_2 capture and injection. The economic profitability of CO_2 sequestration in coal in other basins containing coal with higher methane contents is not addressed in this paper.

Because CO_2 capture/separation cost is the biggest economic driver, knowing what its value would need to be in order to create a favorable economic incentive to inject CO_2 is extremely important. To arrive at this important information, an economic simulation of 1000 Monte Carlo trials was set up and run using the input variable distributions. After each trial, the CO_2 cost yielding a rate of return of 10% (NPV_{10} equal to $0) was calculated and tabulated. The cost of separating CO_2 from the Wyodak PC power plant would need to be less than zero for there to be an economic incentive to inject the CO_2 into an unminable coal seam in the Powder River Basin (see Figure 15). This condition could not be achieved from technological improvements alone, but must be imposed by other outside entities such as a tax on CO_2 emissions or some other incentive. The distribution of CO_2 separation cost required for economical CO_2 sequestration in the Powder River Basin ranges from a low of −$11/ton (12.1/Mg) to a high of $3/ton ($3.3/Mg) with an average separation cost of −$4.36/ton ($4.80/Mg). A CO_2 separation cost of $42/ton corresponds to a total CO_2 cost of $3.03/Mscf ($0.107/m^3). The breakeven CO_2 separation cost of −$4.36/ton (−$4.806/Mg) corresponds to a total cost for CO_2 at the injection site equal to $0.19/Mscf ($0.0067/m^3).

5.6   Summary of economic evaluation

Although injecting flue gas to recover methane from CBM fields may be economic, this method will not significantly contribute to the solution needed to sequester CO_2 in large quantities. A flue gas injection project should be viewed as an enhanced CBM method and not as a realistic option for CO_2 sequestration.

This study suggests that separating CO_2 from flue gas and injecting it into the unminable coal zones of the Powder River Basin seam, while currently uneconomical, can increase recovery of methane by 17% and can sequester over 86,000 tons/ac (192,800 Mg/ha) CO_2.
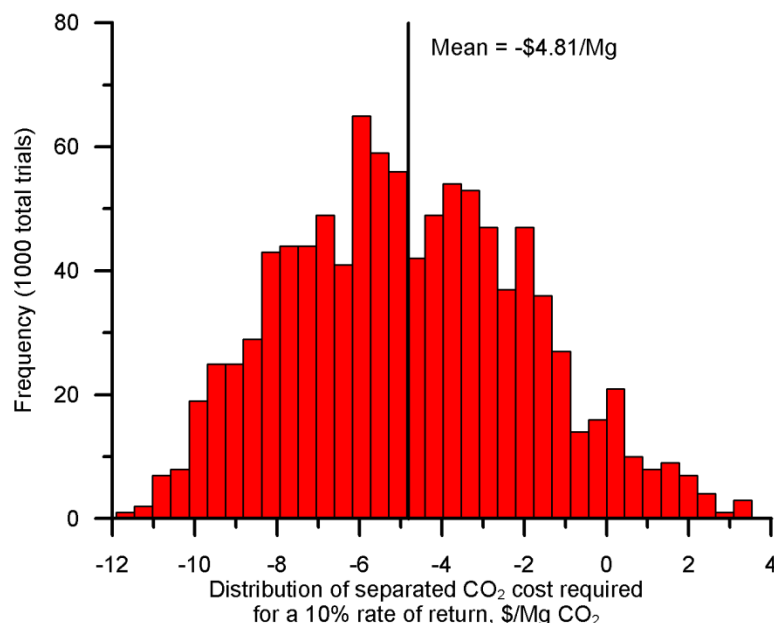
Figure 15. Distribution and mean value of the cost of CO₂ separation/capture required to yield a 10% rate of return.

The cost to separate CO_2 from flue gas was identified as the major cost driver associated with CO_2 sequestration in unminable coal seams in the Powder River Basin. Using existing commercial separations technology, the cost to separate CO_2 from flue gas is currently \$42/ton (\$46.3/Mg) CO_2, which yields a total cost of CO_2 at a sequestration site 50 miles (80.5 km) from the point source equal to \$3.03/Mscf (\$0.107/m^3).

Improvements in separations technology alone are unlikely to drive costs low enough for CO_2 sequestration in unminable coal seams in the Powder River Basin to become economically viable. The average CO_2 separation cost would need to be −\$4.36/ton (−\$4.806/Mg) – corresponding to a total cost of CO_2 of \$0.19/Mscf (\$0.0067/m^3) at a sequestration site – to achieve economic viability for this basin with relatively low gas-content coal.

In order to achieve economic viability, some form of government incentive would need to be imposed to drive the cost to separate CO_2 from flue gas to less than zero. Technological breakthroughs could aid the economics, but would not be expected to accomplish all that is necessary.

6.   References

ALL Consulting, Montana Board of Oil and Gas Conservation, 2004. Coal bed methane primer: new source of natural gas—environmental implications. Contract No. DEFG26-02NT15380, US DOE, National Petroleum Technology Office, Tulsa, Oklahoma, February.

Bank, G.C., Kuuskraa, V.A., 2006. The economics of Powder River Basin coalbed methane development. Prepared for the US DOE by Advanced Resources International, January.

Berkowitz, N., 1985. *Coal Science and Technology 7 – The Chemistry of Coal*, 86. New York City: Elsevier Science.

Bomberger, D.C., Bomben, J.L., Amirbahman, A., Asaro, M., 1999. Nitrogen removal from natural gas: phase II final report. Contract No. DE-AC21-95MC32265, SRI International, Menlo Park California.

Busch, A., Gensterblum, Y., Siemons, N., Krooss, B.M., 2003. Investigation of preferential sorption behaviour of CO_2 and CH_4 on coals by high pressure adsorption/desorption experiments with gas mixtures. 2003 International Coalbed Methane Symposium, University of Alabama, Tuscaloosa, Alabama, 5-9 May, paper 0350.

EIA, 2007. Annual energy outlook 2007 with projections to 2030. US DOE, Energy Information Administration. Report No. DOE/EIA-0383(2007).

Ellis, M.S., Gunther, G.L., Ochs, A.M., Roberts, S.B., Wilde, E.M., Schuenemeyer, J.H., Power, H.C., Stricker, G.D., Blake, D., 1999. Chapter PN: coal resources, Powder River Basin. US Geological Survey Professional Paper 1625-A.

Harpalani, S. and R.A. Schraufnagel, 1990: "Influence of Matrix Shrinkage and Compressibility on Gas Production from Coalbed Methane Reservoirs," SPE paper 20729, presented at the SPE Annual Technical Conference, New Orleans, LA.

Hendriks, C., Graus, W., van Bergen, F., 2004. Global carbon dioxide storage potential and costs. ECOFYS, Utrecht, The Netherlands. Report No. EEP-02001.

Liang, J.T., Raterman, K.T., Robertson, E.P., 2003. A mechanistic model for CO_2 sequestration in tiffany coal bed methane field. 2003 International Coalbed Methane Symposium, University of Alabama, Tuscaloosa, Alabama, 5-9 May, paper 0339.

Mathews, J.P., Karacan, O., Halleck, P., Mitchell, G.D., Grader, A., 2001. Storage of pressurized carbon dioxide in coal observed using X-ray tomography. First National Conference on Carbon Sequestration, Washington, D.C., 14-17 May.

Mavor, M.J., Gunter,W.D., Robinson, J.R., 2004. Alberta multiwell micro-pilot testing for cbm properties, enhanced methane recovery and CO_2 storage potential. 2004 SPE Annual Technical Conference and Exhibition, Houston, Texas, 26-29 September, paper SPE 90256.

Nelson, C.R., Steadman, E.N., Harju, J.A., 2005. Geologic CO_2 sequestration potential of the Wyodak-Anderson coal zone in the Powder River Basin. Plains CO_2 Reduction (PCOR) Partnership Topical Report for U.S. Department of Energy; Energy and Environmental Research Center: University of North Dakota, August.

Palmer, I. and J. Mansoori: "How Permeability Depends on Stress and Pore Pressure in Coalbeds: A New Model," paper SPE 52607, *SPE Reservoir Evaluation & Engineering* (December 1998) 539-544.

Pekot, L.J., Reeves, S.R., 2003. Modeling the effects of matrix shrinkage and differential swelling on coalbed methane recovery and carbon sequestration. 2003 International Coalbed Methane Symposium, University of Alabama, Tuscaloosa, Alabama, 5-9 May, paper 0328.

Prusty, B.K., Harpalani, S., 2004. A Laboratory study of methane/CO_2 exchange in an enhanced CBM recovery scenario. 2004 International Coalbed Methane Symposium, University of Alabama, Tuscaloosa, Alabama, 12-14 May, paper 0426.

Puri, R., Yee, D., 1990. Enhanced coalbed methane recovery. 1990 SPE Annual Technical Conference and Exhibition, New Orleans, Louisiana, 23-26 September, paper SPE 20732.

Reeves, S.R., 2003. Assessment of CO_2 sequestration and ECBM potential of US coalbeds. US DOE topical report No. DE-FC26-00NT40924, February.

Reeves, S., Taillefert, A., Pekot, L., Clarkson, C., 2003. The Allison unit CO_2-ECBM pilot: a reservoir modeling study. US DOE topical report No. DE-FC26-0NT40924, February.

Robertson, E.P., 2005. Measurement and modeling of sorption-induced strain and permeability changes in coal. Ph.D. Thesis, Colorado School of Mines, Golden, Colorado, December; also published as an external report from Idaho National Laboratory, INL/EXT-06-11832, October.

Robertson, E.P., 2007. Analysis of CO_2 separation from flue gas, pipeline transportation, and sequestration in coal. Idaho National Laboratory external report No. INL/EXT-08-13816, Idaho Falls, Idaho, September.

Robertson, E.P. and Christiansen, R.L., 2007. Modeling laboratory permeability in coal using sorption-induced strain data. *SPE Reservoir Evaluation & Engineering* **10** (3), 260–269.

Robertson, E.P. and Christiansen, R.L., 2007 (a). Methods and Apparatus for Measurement of a Dimensional Characteristic and Methods of Predictive Modeling Related Thereto. U.S. Patent No. US 7,224,475.

Robertson, E.P. and Christiansen, R.L., 2007 (b). Methods for Measurement of a Dimensional Characteristic and Methods of Predictive Modeling Related Thereto. U.S. Patent No. US 7,284,604 B2.

Robertson, E.P. and Christiansen, R.L., 2008. A permeability model for coal and other fractured, sorptive-elastic media. *SPE Journal*, September, 314-324.

Schroeder, K., Ozdemir, E., Morsi, B.I., 2002. Sequestration of carbon dioxide in coal seams. J. Energy & Environment Research 2, 54–63 1.

Seidle, J.P. and L.G. Huitt, 1995: "Experimental Measurement of Coal Matrix Shrinkage Due to Gas Desorption and Implications for Cleat Permeability Increases," paper SPE 30010, presented at the SPE international Meeting on Petroleum Engineering, Beijing, China (14-17 November).

Shi, J.Q. and S. Durucan: "Changes in Permeability of Coalbeds During Primary Recovery – Part 1: Model Formulation and Analysis," paper 0341 proc. at the 2003 International Coalbed Methane Symposium, University of Alabama, Tuscaloosa, Alabama (May 2003).

Steinberg, M., 2001. Decarbonization and sequestration for mitigating global warming. First National Conference on Carbon Sequestration, Washington, D.C., 14-17 May.

Stevens, S.H., Spector, D., Riemer, P., 1998. Enhanced coalbed methane recovery using CO_2 injection: worldwide resource and CO_2 sequestration potential. 1998 SPE International Conference and Exhibition in China held in Beijing, China, 2-6 November, paper SPE 48881.

Thomas, C.P., Doughty, T.C., Hackworth, J.H., North, W.B., Robertson, E.P., 1996. Economics of Alaska north slope gas utilization options. Idaho National Laboratory external report No. INEL-96/0322, Idaho Falls, Idaho, August, B-8.

U.S. DOE, 2007a. Electric power annual — with data for 2006. US DOE — EIA, 22 October. Available online at: http://www.eia.doe.gov/cneaf/electricity/epa/epa_sum.html.

U.S. DOE, 2007b. 2007 coal power plant database. US DOE – National Energy Technology Laboratory, 16 November. Available online at: http://www.netl.doe.gov/publications/ press/2007/07079-Coal_Plant_Database_Available.html.

van Bergen, F., Pagnier, H.J.M., van der Meer, L.G.H., van den Belt, F.J.G., Winthaegen, P.L.A., Krzystolik, P., 2003. Development of a field experiment of ECBM in the Upper Silesian coal basin of Poland (RECOPOL). 2003 International Coalbed Methane Symposium, Tuscaloosa, Alabama, 5-9 May, paper 0320.

White, C.M., Smith, D.H., Jones, K.L., Goodman, A.L., Jikich, S.A., La Count, R.B., DuBose, S.B., Ozdemir, E., Morsi, B.I., Schroeder, K.T., 2005. Sequestration of carbon dioxide in coal with enhanced coalbed methane recovery—a review. Energy & Fuels 19 (3), 659–724.

Zutshi, A., Harpalani, S., 2004.Matrix swelling with CO_2 injection in a cbm reservoir and its impact on permeability of coal. Paper 0425 presented at the 2004 International Coalbed Methane Symposium, University of Alabama, Tuscaloosa, Alabama, 12-14 May.